Experimental Study on Punching Shear Behavior of Crushed Clay Brick Lightweight Concrete Flat Plate Slabs

Mohamed Hossiny[1,2*], Mohamed Abd Elrahman[2], Salah E. El-Metwally[2]
[1] Delta Higher Institute for Engineering and Technology, Mansoura, Egypt.
[2] Structural Engineering Department, Mansoura University, Mansoura, Egypt.
[*] Corresponding author Email: eng.m.hossiny@gmail.com

Abstract

This paper presents an experimental investigation on the behavior of crushed clay brick (CCB) lightweight concrete (LWC) flat plate slabs under punching load. The CCB resulting from either the building process or the remnants of brick factory production lines constitutes one of the most notable wastes in the world, which motivated many researchers exploring its usage as an alternative to natural aggregates. Six LWC slabs were constructed from CCB as coarse and fine aggregates in addition to crushed brick powder (CBP). The produced concrete had a compressive strength of 25, 28, and 32 MPa and a dry density of less than 1800 kg/m^3. The tested slabs were divided into three groups (A, B, and C) according to the compressive strength. Each group had included two different tension reinforcement ratios of 0.428 and 0.616%. Based on the test results, the effect of the lightweight aggregates (LWA) was discussed and compared to codes' prediction of punching capacity. These codes include the ACI-318-19, EC-2, the Canadian code CSA-2004, ECP-203-2017, and the JSCE-2007. From the test results, it was found that the surface of punching shear failure of the tested slabs extended a distance ranged from 2.3 to 3.3 times the slab thickness measured from the column face, with the shear plane inclined at 20.3° to 27.4° to the plane of the slab. In addition, the punching shear strength can be fairly predicted by the selected international codes.

Keywords

crushed clay brick; lightweight concrete; flat plate slabs; slab-column connection; punching shear.

1. Introduction

Punching failure in reinforced concrete flat plates is a brittle failure caused by diagonal shear cracks developed through the slab thickness forming a frustum pyramid in rectangular columns and a truncated cone in case of circular columns. Many factors affect the punching capacity of slabs such as concrete strength, column-to-slab aspect ratio, flexural reinforcement, shear reinforcement and boundary conditions. Design codes deal with the punching failure problem in different ways, e.g., ACI-318-19 [1], EC-2 [2], Canadian code CSA-2004 [3], ECP-203 2017 [4], and JSCE-2007 [5]. Reducing the reinforced concrete slab's weight is one of the common solutions to the slab-column connection problem. Lightweight aggregate concrete (LWC) slabs were tested for punching shear strength by Clarke [6] using Lytag, Perlite, Leca, Fibo, and Liapor as lightweight aggregates with dry density of less than 2000 kg/m^3. The normal weight aggregates, which were obtained from the Thames Valley (U.K), were taken as a reference for comparison. The experimental results indicated that the dry densities ranged from 85 percent to 65 percent of normal-weight concrete. The slabs constructed from LWC were up to 30% stronger in punching shear than those made with the reference aggregate when normalized to their densities.

Kim et al. [7] investigated the punching shear behavior of the LWC slab by using several types of lightweight aggregate (clay, shale and slate) and forms (crushed or spherical shape). According to their test results, the punching shear failure surface of the LWC slab with spherical-shaped coarse aggregate was less inclined with the slab plane than that of the LWC slab with crushed-shaped coarse aggregate, resulting in an increase in the punching shear strength of the slab. On the other hand, the failure surface of LWC slab with crushed shape coarse aggregate and coarse aggregate with normal shape had similar inclination angle. Osman et al. [8] tested five slabs made with high-strength lightweight concrete under punching load; the results indicated that the surface of punching shear failure of the tested slabs extended a distance of about 3.17 times the slab thickness measured from the column face, with the shear plane inclined at an angle 25° to 29° to the slab plane.

LWC may be designed to meet a wide range of needs, from a low-density concrete for insulation to a high-strength concrete for structural purposes. Sahoo et al. [9] studied the punching shear behavior of concrete slabs with recycled aggregate with replacement levels of 0%, 50%, and 100%. The experimental results indicated that the punching shear increased with increasing the compressive strength, and the main punching shear crack was inclined to the horizontal with an angle in the range of 28^o–33^o. Urban et al. [10] investigated punching shear strength of LWC slabs with dry densities of less than 1800 kg/m^3 and the tests indicated that the punching shear cracks were inclined to the horizontal with an angle in the range of 20^o–40^o.

Crushed Clay Brick (CCB) is a type of aggregate used as a lightweight aggregate and is abundant as waste from brick factories, found in large quantities all over the world. There is a promising way to reuse this waste as lightweight aggregate and to preserve the environment. Upon crushing and sieving e CCB, fine and coarse lightweight aggregate can be obtained. CCB can also be ground into a powder to increase its surface area and enhance its pozzolanic activity for use as a partial replacement of cement [11]–[14]. Several studies have investigated CCB as an alternative to natural aggregates in different forms in concrete. Several studies used bricks as coarse aggregate[11], [15], [24]–[31], [16]–[23], some used it as fine aggregate [31], [32] and others benefited from the pozzolanic reaction resulting from the use of CCB as a powder with an alternative ratio of cement to reduce the cement content [33], [34], [43], [35]–[42]. Atyia et al. [44] used crushed clay powder which passed through 0.125 mm, as partial replacement of cement and concluded that CBP has a positive effect on the concrete strength at later ages. Some researchers used CCB as fine and coarse aggregate with 100% replacement for natural aggregates [22], [31], [44]–[47]. From all previous studies that used CCB in concrete, it is possible to obtain lightweight concrete with a dry density of less than 2000 kg/m^3 and a compressive strength greater than 20 MPa, suitable for construction purposes according to the ACI 213R-14 [48] and a tensile strength greater than 2.0 MPa. From what was referred to in research and studies, attention was focused on improving the mechanical and physical properties of concrete from crushed bricks without compromising the behavior of this type of concrete in structural elements, including flat slabs, which made it a subject of interest for this research.

In this research, crushed bricks are used as coarse and fine aggregate, and also as a filling powder as a filler, as a partial alternative form of aggregate to improve workability and concrete strength, for the sake of obtaining LWC with a dry density of less than 1800 kg/m^3 and a compressive strength higher than 25 MPa. In this study, the obtained concrete is used to construct flat plates and the behavior of such structural elements under punching load is investigated. In addition, the applicability of international codes for the prediction of the punching shear behavior of flat plate slabs from CCB lightweight concrete is examined.

2. Experimental program

The experimental program considering testing six squared lightweight concrete flat plate specimens is shown in Fig. 1. The specimens were divided into three groups (A, B, and C) according to the compressive strength of concrete (f_{cu}). Each group had the same compression reinforcement, but the tension reinforcement was variable.

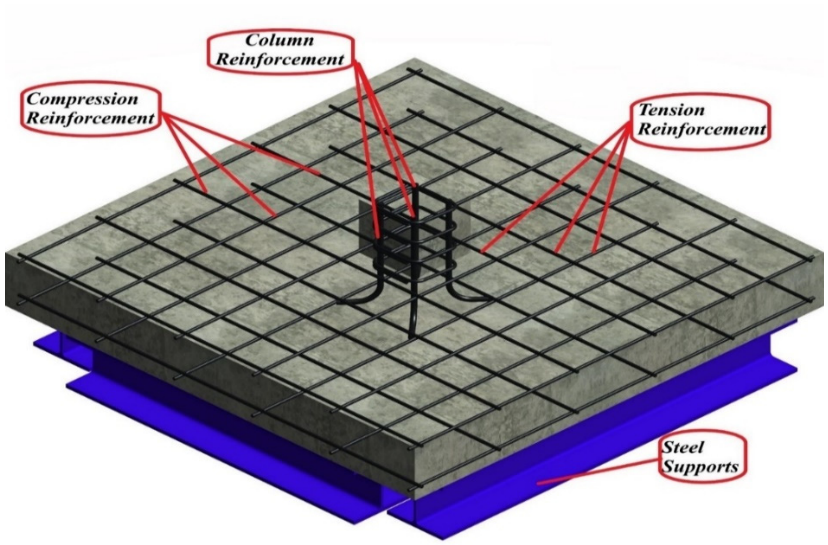

Fig. 1 Specimen layout.

2.1 Materials

2.1.1 Concrete

One of our targets was to employ available sustainable material as aggregate to produce lightweight concrete; hence, the crushed clay brick (CCB) aggregate was selected. The used CCB was collected from brick factories in Egypt as shown in Fig. 2. It, as shown in Fig. 3, was grinded and sieved manually to produce coarse aggregate (CCBA) with particle size ranging from 5-10 mm, fine aggregate (FCBA) with particle size ranging from 250 µm to 5 mm and crushed clay powder (CCP) with particle size less than 250 µm, used as an aggregate replacement (15 %). For all types of aggregates, tests were carried out according to the ECP 203-2017 [4] criteria. The physical properties of the used aggregates are shown in Table 1. The used cement was CEM I 52.5N Portland cement complying with the ECP 203-2017 criteria, and with specific gravity of 3.05 g/cm^3. Silica fume and superplasticizer (Sikament 163M complies with ASTM C-494 Type A&F and BS 5075 part 3) was used to enhance the compressive strength and to maintain the slump of fresh LWC at the same level. Air entraining admixture (ADDICRETE LP complying with ASTM C 260 and EN 934 - 2 with specific gravity of 1.02 ± 0.01) were used to reduce the dry density of concrete. The grading of CCBA, FCBA, CCP and Cement are shown in Fig. 4.

Fig. 2 Sample of brick factories, Egypt.

(a) CCBA

(b) FCBA

(c) CBP

Fig. 3 Crushed clay brick: (a) coarse aggregate; (b) fine aggregate; and (c) powder.

Table 1 Physical properties of the used aggregates

Aggregates	CCBA	FCBA
Specific Gravity (gm/cm^3)	2.12	2.12
Bulk Density (kg/m^3)	1025	1170
Water Absorption (%)	13	16.5

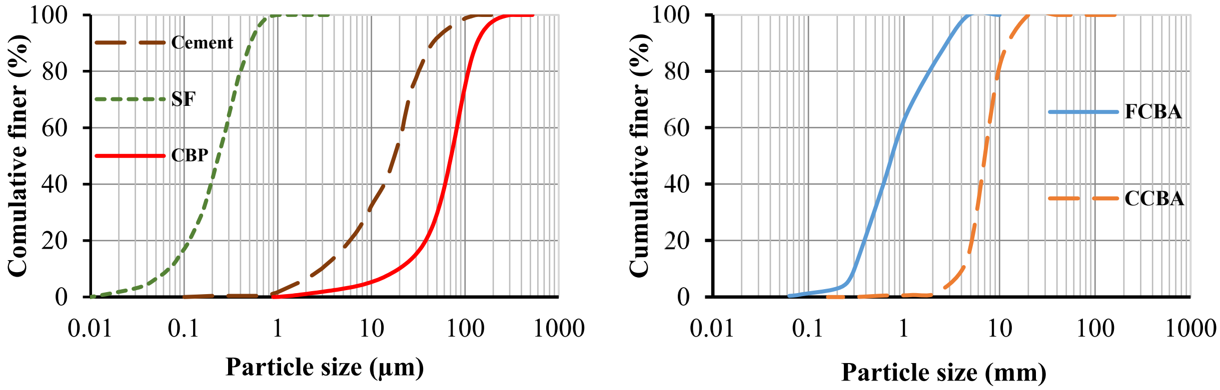

Fig. 4 Particle size distributions of materials (cement, SF, CBP, FCBA, and CCBA).

2.1.2 Concrete mix design

The considered specimens were constructed from three different types of crushed clay brick lightweight concrete mixes with the properties given in Table 2 and designed using the absolute volume method in order to obtain cube compressive strength ranging from 25 to 32 MPa after 28 days. The aggregate was used in its dry state and the mixing water was increased by the amount needed for absorption for each type of aggregate. Five 0.035 m^3 batches, from a mixer with capacity 0.05 m^3, were used to cast each specimen. Each specimen was placed onto wooden formwork and an external mechanical vibrator was used. For each specimen, three cylinders Ø150/300 mm, three cylinders Ø100/200 mm, three cubes 150*150*150 mm, and three cubes 100*100*100 mm size) were cast. The casting procedure is illustrated in Fig. 5. The cubes and cylinders were tested to obtain the compressive and tensile strengths and the stress-strain curves of each mix as shown in Figs. 6 and 7 and Table 3.

(a) Specimens **(b) Cylinders and cubes.**

Fig. 5 Finishing of specimens.

(a) Two halves of a cylinder specimen after tension test.

(b) Cube specimens after compression test.

Fig. 6 Cube and cylinder after test.

Table 2 Concrete mix components, kg/m^3

Mix no.	W/C	Cement	SF	Water	Water for absorption	SP	CA	FA	CCP 15% agg.	AEA, kg/m^3	AEA %
M0										0	0%
M30	0.48	432	48	230	79	10	535.5	510	184.5	1.44	0.30%
M120										5.76	1.20%

SF: Silka fume; SP: Superplasticizer; CA: Coarse aggregate; FA: Fine aggregate, AEA: Air entraining admixture.

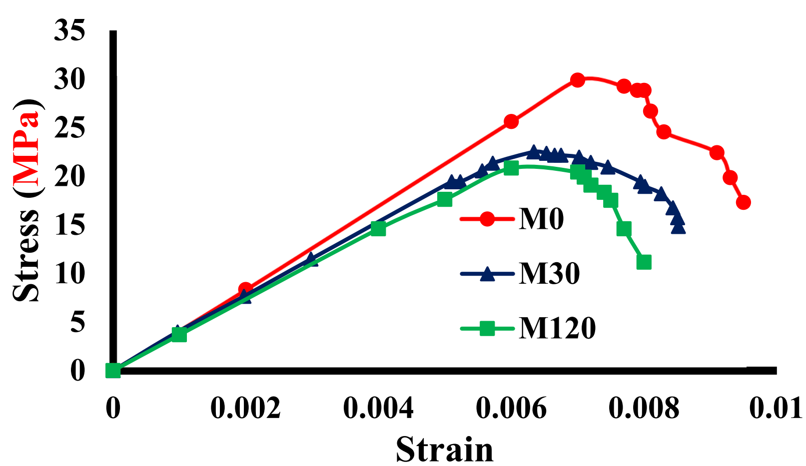

Fig. 7 Stress strain curve of LWC.

Table 3 Mechanical properties of lightweight concrete

Mix No.	Dry density, kg/m^3	Compressive strength, MPa				Tensile strength, MPa	Slump, mm	Strength/Density Ratio
		7 days Cube 10*10 cm	28 days Cube 10*10 cm	28 days Cylinder 15*30cm	28 days Cube 15*15cm			
M0	1787	30.5	37.3	29.0	32.0	2.67	105	2.09
M30	1710	26.8	33.3	21.0	28.1	2.02	130	1.95
M120	1610	24.0	30.5	20.3	24.9	2.00	175	1.55

2.2 Reinforcement

Normal mild steel was used for compression reinforcement and column stirrups, while high-grade steel was used for tension reinforcement and column reinforcement. The normal mild steel had a yield stress, $f_y = 240MPa$, and ultimate strength, $f_u = 356MP$, whereas the high-grade steel had, $f_y = 520MPa$, and ultimate strength, $f_u = 650MP$a. Both types of steel had a modulus of elasticity $E_y = 2 \times 10^5\ MPa$, and Poisson's ratio = 0.3.

2.3 Test specimens

Six squared lightweight concrete flat plate specimens presented in three groups (A. B, and C) with three different concrete strengths f_{cu}, equal to 32, 28 and 25 MPa, respectively, were considered. For the tension (bottom) reinforcement, each group had two different ratios, 0.428% and 0.616%, uniformly distributed both ways; 6 bars per section. The reinforcement was distributed uniformly throughout the width of the slab. All slabs had bottom and top layers of bars at a uniform spacing 210 mm from center to center in both orthogonal directions. The top reinforcement was 8 mm diameter, and the bottom bars were 10 mm and 12 mm according to the slab group. The column reinforcement was four bars of 12 mm diameter and three stirrups with 8mm diameter. The reinforcement layout and specimens' details are shown in Fig. 8 and Table 4.

Table 4 Details of test specimens

Group	Specimens	f_{cu} (MPa)	Column Size (mm)	Effective Depth (mm)	Tension steel %	Compression steel %
A	A0	32	150*150	100	0.428(6D10/sec)	0.2743(6D8/sec)
	A1				0.616(6D12/sec)	
B	B0	28			0.428(6D10/sec)	
	B1				0.616(6D12/sec)	
C	C0	25			0.428(6D10/sec)	
	C1				0.616(6D12/sec)	

f_{cu} is the strength of standard cube 150 mm, Sec: Section

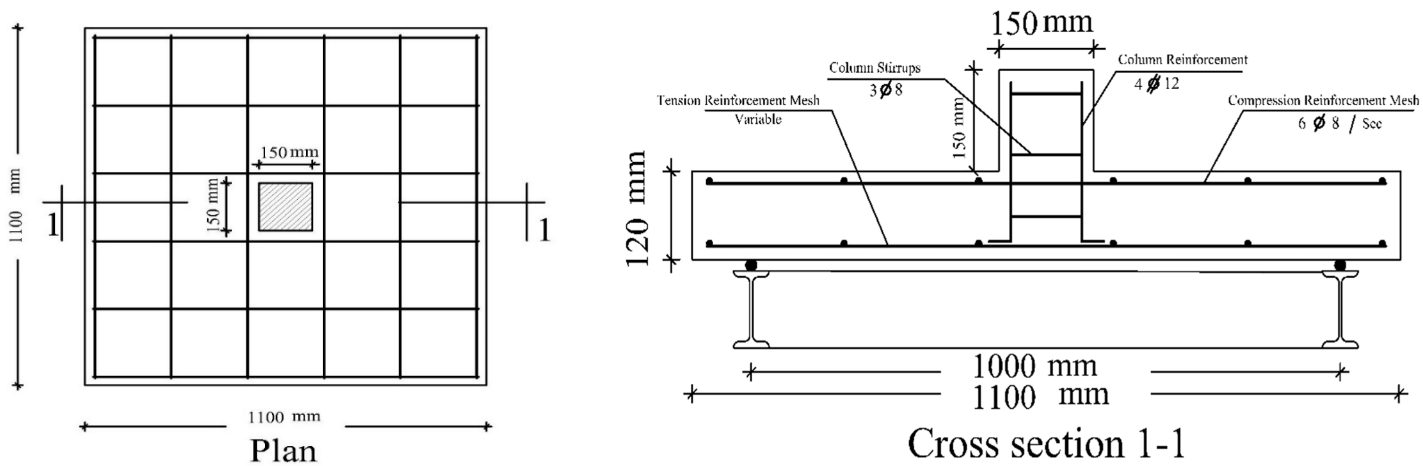

Fig. 8 Typical steel arrangement details of slabs.

2.4 Test setup

The specimens were placed centered below the hydraulic jack on a horizontal squared frame (IPE No. 150), and four steel bars (25 mm dia.) were welded on the top surface of the square frame to make sure that the supports under the specimens are pinned. The description and photos of the loading system and test setup are shown in Figs. 9 and 10.

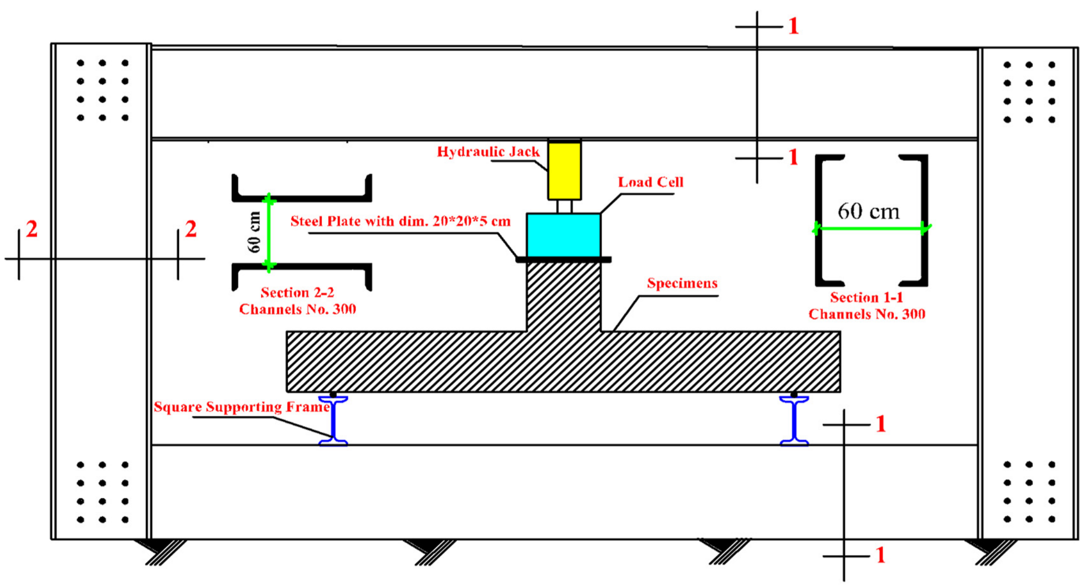

Fig. 9 Test setup.

Fig. 10 Photos of test setup.

3. Results and discussion

3.1 Effect of concrete strength on punching shear strength

From the results in Table 5 and Fig. 11, it can be noted that reducing the concrete strength from 32 MPa to 28 MPa, led to about 20% and 17% reduction in the ultimate punching load of specimens with tension reinforcement ratios of 0.428% and 0.616%, respectively. Reducing the concrete strength from 28 MPa to 25 MPa, led to about 10% and 2% reduction in the ultimate punching load of specimens with tension reinforcement ratios of 0.428% and 0.616%, respectively.

Table 5 Summary of experimental results

Specimens	Exp. P_u (kN)	Angle of punching	Diameter of punching (mm)	First cracking load (kN)
A0	245.52	20.27	800	65
A1	255.4	20.97	776	65
B0	197.268	22.78	723	62
B1	211.628	24.24	683	62
C0	178.15	24.65	673	48
C1	206.43	27.35	614	60

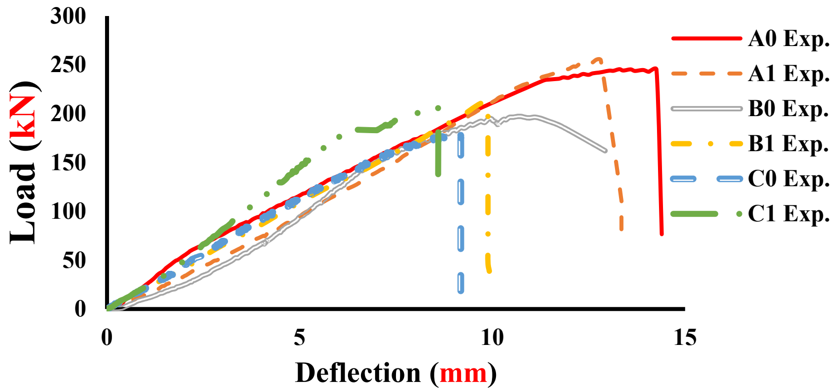

Fig. 11 Load-deflection curve of tested specimens.

3.2 Cracking behavior

For all specimens, cracks had been observed and marked during the test. In all specimens, the initial crack development followed a similar pattern. First, diagonal cracks occurred near the column at a load of about 60.0 kN. At a loading from 60.0-130.0 kN cracks grew towards the middle distance between the column and the slab support in all directions and new diagonal cracks had initialed. At a loading above 130 kN and up to failure, all diagonal cracks were getting wider and radial cracks had developed. Fig. 12 shows the crack pattern in the tension side of the specimens. For the compression side, cracks had developed around the column in all the specimens as shown in Fig. 13.

Specimen (A0) **Specimen (A1)**

Fig. 12 The crack pattern in the tension side of all specimens.

(c) Specimen (B0)

(d) Specimen (B1)

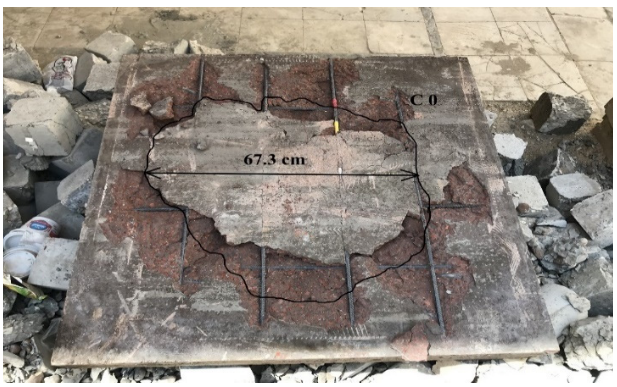

(e) Specimen (C0)

(f) Specimen (C1)

Fig. 12 Contd.

Fig. 13 The crack pattern in the compression side around the columns of specimens A0 and A1.

3.3 Tension reinforcement strains

Strain gauges (with electrical resistance 10 mm length strain) were affixed to the steel reinforcement to measure the strains in areas of particular interest. The selected locations of strain gauges are illustrated in Fig. 14.

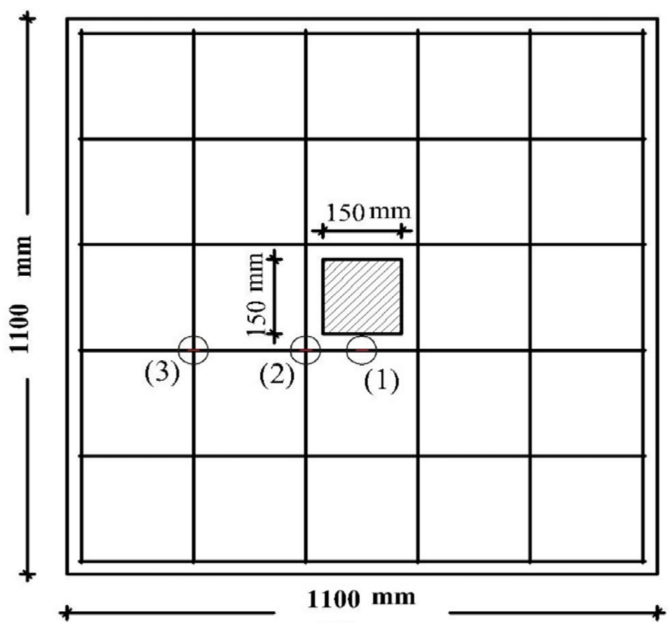

Fig. 14 Positions of strain gauges of tension steel.

Fig. 15 shows the load-tension reinforcement strain curves of all specimens at positions (1), (2), and (3). The results show that the flexural steel of all specimens reached the highest value in position (1) and reached the yield point at 74%, 58%, 91%, 80%, 83%, and 61% of ultimate load for specimens A0, A1, B0, B1, C0, and C1 respectively. For these specimens also, the steel reached the yield point in position (2) at 78%, 76%, 93%, 81%, 85%, and 68% of ultimate load. On the other hand, the steel in position (3) did not yield in specimens A1, C0, and C1, but reached the yield point at 96% of ultimate load for specimen B1 and 92% for specimens A0 and B0, respectively.

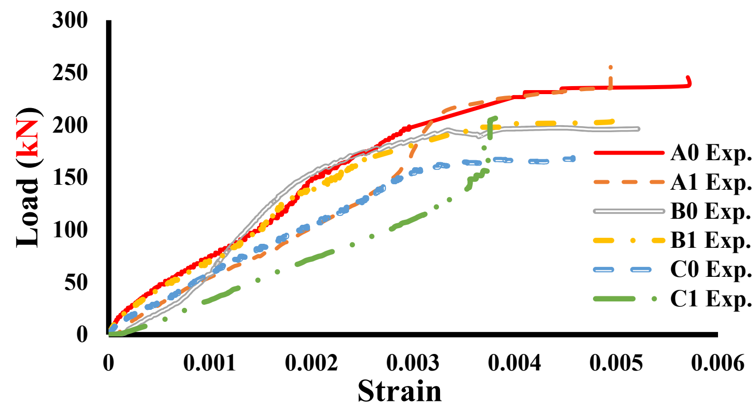

(a) Strain gauges of position (1)

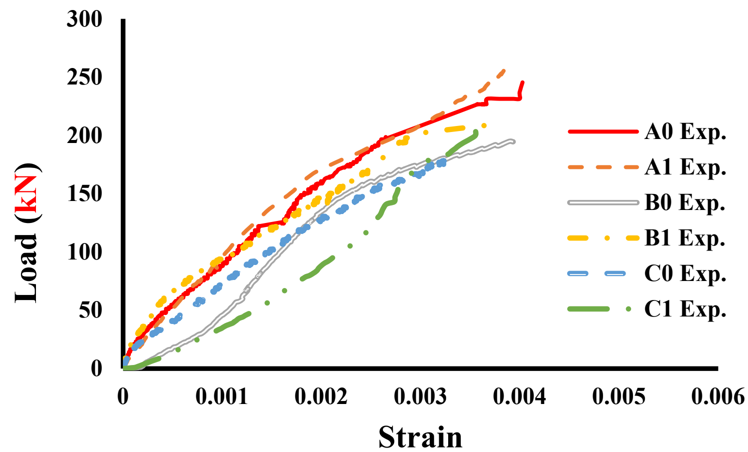

(b) Strain gauges of position (2)

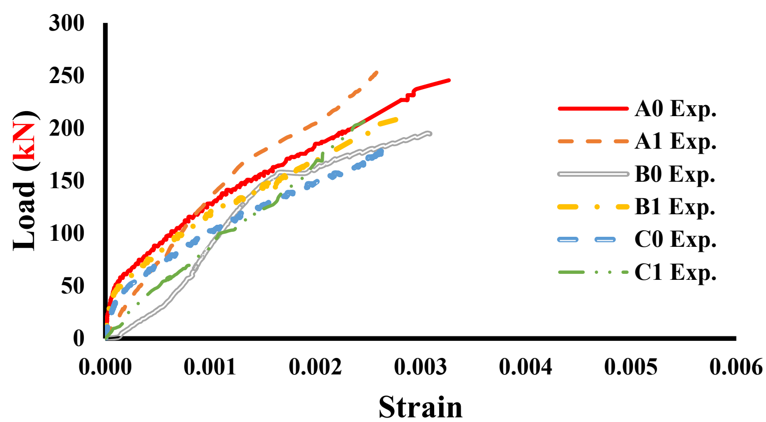

(c) Strain gauges in position (3)

Fig. 15 Load-strain curve of tensile steel of slabs.

4. Codes prediction of ultimate punching load

In this section, the nominal punching shear capacity (setting the strength reduction factors equal to one) of slab-column connection of the tested specimens is re-predicted using the provisions of some selected building codes. The American code (ACI 318-19) and the Canadian code (CSA 2004) account for the weight of concrete slab, while as other codes, such as the Egyptian code (ECP-203-2017), the Euro code (EC-2), and the Japanese (JSCE-2007) code, do not. The predicted nominal strength values from the selected codes are briefly presented, and the obtained results are given along with the test results in Table 6.

4.1 ACI 318-19 code

In the ACI 318-19 code [1], the loaded region is 0.50*d* away from the critical section. The design is based on:

$$\nu_u < \phi \ \nu_c \tag{1}$$

$$\nu_u = \frac{V_u}{b_0 d} \tag{2}$$

where ϕ is the strength reduction factor, equal to 0.85, ν_u is the applied shear stress in the absence of moment transfer due to a factored shear force V_u and b_o is the perimeter of the critical section. The nominal punching shear strength is the smallest of the following three values (in SI units):

$$\nu_c = 0.17\lambda\sqrt{f_c'}\ [1 + \frac{2}{\beta_c}] \quad (\mathrm{N/mm^2}) \tag{3a}$$

$$\nu_c \le 0.083\lambda\sqrt{f_c'}\ [2 + \frac{\alpha_s d}{b_o}] \quad (\mathrm{N/mm^2}) \tag{3b}$$

$$\nu_c \le 0.33\lambda\sqrt{f_c'} \quad (\mathrm{N/mm^2}) \tag{3c}$$

where α_s is a factor taken as 40, 30 and 20 for interior column, edge and corner columns, respectively, λ is a factor to account for low density (is equal to 0.75 for lightweight concrete), d is the average effective depth, b_o is the perimeter of critical section, f_c' is the cylinder compressive strength of concrete and β_c is the ratio of the larger to the smaller side of the column section.

4.2 EC-2 code

As seen in Fig. 16, the EC-2 code [2] critical section is located at a distance 2*d* from the column face or loaded region. Similarly, the shear stress, ν_f on the control section should not be greater than the shear resistance, ν_r, where for rectangular columns, the basic control section includes round corners.

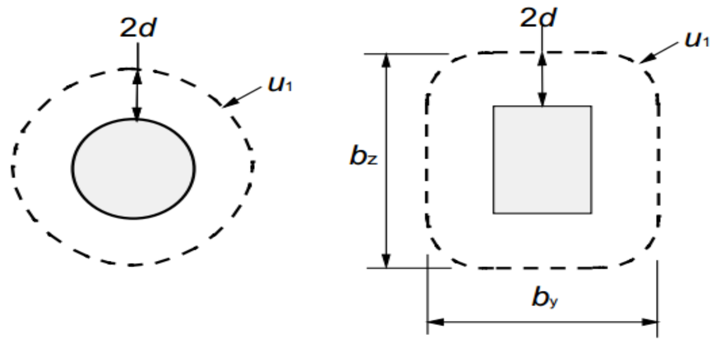

Fig. 16 Typical basic control perimeters around loaded areas.

For interior and exterior slab-column connections without shear reinforcement, the shear resistance ν_r for the basic control section is calculated as follows:

$$\nu_r = \frac{0.18}{\gamma_c} k(100\rho_1 f_{ck})^{1/3} > \nu_{min} \tag{4}$$

$$k = 1+\sqrt{\frac{200}{d}} \leq 2.0 \textit{ and } d, \textit{ in (mm)} \tag{5}$$

where f_{ck} is the characteristic concrete strength in MPa, $\rho_1 = (\rho_z \rho_y)^{0.5} < 0.02$, ρ_z and ρ_y are the reinforcement ratios in the *z* and *y* directions, respectively, for a slab width equals to the column width plus 3*d* each side, *d* is the slab thickness in mm, and γ_c is the strength reduction factor of concrete and is equal to 1.5.

$$\nu_{min} = 0.035k^{2/3} f_{ck}^{0.5} \quad (\text{N/mm}^2) \tag{6}$$

4.3 CSA-2004 code

The 2004 edition of the Canadian code CSA-2004 [3] is very similar to the ACI 318-19 in many respects. In the absence of shear reinforcement, the punching shear strength of the concrete is the smallest of the following three values.

$$\nu_c = 0.20\lambda\sqrt{f_c'}\ \phi_c[1 + \frac{2}{\beta_c}] \quad (\text{N/mm}^2) \tag{7}$$

$$\nu_c \leq 0.20\lambda\sqrt{f_c'}\ \phi_c[2 + \frac{\alpha_s d}{0.20 b_o}] \quad (\text{N/mm}^2) \tag{8}$$

$$\nu_c \leq 0.38\lambda\phi_c\sqrt{f_c'} \quad (\text{N/mm}^2) \tag{9}$$

where β_c is the ratio of long to short side of column, $(\alpha_s/0.20)$ equals to 20, 15, and 10 for interior columns, edge columns and corner columns, respectively, λ is a factor to account for low density (is equal to 0.75 for lightweight concrete), and ϕ_c is the material reduction factor (is equal to 0.60).

4.4 ECP-203-2017 code

The ECP-203-2017 [4] allows the treatment of the punching problem by either one of two different methods. The first leads to accurate calculations of the unbalanced moment over the column, and this method is like the ACI 318-19 approach. The last method adopts simplified calculations, which is used in this study, where the punching shear stresses are magnified in order to account for the unbalanced moment transfer to columns. The increase in stresses is 15%, 30% and 50% for interior, edge and corner connections, respectively. The shear stress, q_u, is given by:

$$q_u = \frac{Q_{up}\beta}{b_o d} \qquad (\text{N/mm}^2) \qquad (10)$$

where Q_{up} is the ultimate design shear force, β is the magnification factor, equals to 1.15 for interior connection, b_o is the critical shear perimeter and d is the effective slab depth.

The shear stress, q_u, should not exceed the punching shear strength, q_{cup} , which is the smallest of the following three values:

$$q_{cup} = 0.8x\left(\frac{\alpha\ d}{b_o} + 0.20\right)\ x\ \sqrt{\frac{f_{cu}}{\gamma_c}} \qquad (\text{N/mm}^2) \qquad (11a)$$

$$q_{cup} = 0.316x\left(\frac{a}{b} + 0.50\right)\ x\ \sqrt{\frac{f_{cu}}{\gamma_c}} \qquad (\text{N/mm}^2) \qquad (11b)$$

$$q_{cup} = 0.316\ x\ \sqrt{\frac{f_{cu}}{\gamma_c}} \qquad (\text{N/mm}^2) \qquad (11c)$$

where α : is the factor taken equal to 4, 3, and 2 for interior and corner, respectively, f_{cu} is the standard cube characteristic strength, γ_c is the reduction factor of concrete, *a* is the smaller dimension of the column, and *b* is the larger dimension of the column.

4.5 JSCE-2007 code

The critical section of the JSCE-2007 code [5] is placed at 0.50d away from the loaded area. The punching shear capacity of reinforced concrete slabs, ν_u, can be predicted using the following equations:

$$\nu_u = \beta_d \beta_p \beta_r f_{pcd} u_p d \qquad (\text{N/mm}^2) \qquad (12)$$

$$f_{pcd} = 0.20\sqrt{f_c'} \qquad (\text{N/mm}^2) \qquad (13)$$

$$\beta_d = \left(\frac{100}{d}\right)^{1/4} \tag{14}$$
$$\beta_p = (100\,\rho)^{1/3} \tag{15}$$
$$\beta_r = 1 + \frac{1}{1+0.25u/d} \tag{16}$$
$$u_p = u + \pi d \qquad \text{(mm)} \tag{17}$$

where f_c' is the cylinder compression strength of concrete (MPa), d is the average effective depth (mm), ρ is the average tension steel reinforcement ratio, u is the perimeter of the loading pad (mm), and u_p is the perimeter of the critical section located at a distance of $0.50d$ from the edge of the loading pad (mm). The values of f_{pcd}, β_d , and β_p are limited to 12 N/mm^2, 1.50 and 1.50, respectively.

Table 6 Comparison between codes predictions and test results

Specimens	**Exp. P_u, kN**	**Code P_u, kN**					**Exp. P_u / Code P_u**				
		ACI	**EC**	**CSA**	**ECP**	**JSCE**	**ACI**	**EC**	**CSA**	**ECP**	**JSCE**
A0	245.5	206	221	242	222	211	1.19	1.11	1.01	1.11	1.17
A1	255.4	206	221	242	222	238	1.24	1.15	1.05	1.15	1.07
B0	197.3	175	199	206	207	179	1.13	0.99	0.96	0.95	1.10
B1	211.6	175	199	206	207	202	1.21	1.06	1.03	1.02	1.05
C0	178.2	172	197	203	196	176	1.03	0.91	0.88	0.91	1.01
C1	206.4	172	197	203	196	199	1.20	1.05	1.02	1.05	1.04
					Average		1.17	1.05	0.99	1.03	1.07

4.6 Comparison

The predicted nominal punching shear strength of the tested specimens by the selected building codes along with test results are given in Table 6. Obviously, the considered codes can be fairly utilized in the design of the LWC flat plates for punching. Nevertheless, the ACI 318-19 prediction is conservative.

5. Conclusions

Based on the results obtained from this experimental study on the punching shear behavior of lightweight concrete made by crushed clay brick aggregate, the following conclusions can be drawn:

1. The crushed clay brick (CCB) aggregate can be used as a replacement of normal aggregate to produce lightweight concrete (LWC) with dry density ranging from 1610 to 1780 kg/m^3.
2. The CCB concrete can be considered a structural lightweight concrete since it has a compressive strength higher than 25 MPa.
3. Increasing the flexural reinforcement ratio has a significant effect on increasing the punching shear strength capacity by 4% to 15 % according to the concrete compressive strength.
4. Punching shear failure in tested crushed clay brick LWC flat plate slabs is preceded by yielding of tension steel reinforcement and is accompanied by cracks mainly in the radial direction and partly in the circumferential direction.
5. The surface of punching shear failure of the tested flat plate slabs extended a distance ranging from 2.3 to 3.3 times the slab thickness measured from the column face, with the shear plane inclined at 20.3° to 27.4° to the plane of the slab.
6. The punching shear strength can be fairly predicted by many international building codes, e.g., the ACI 318-19, CSA 2004, ECP-203-2017, EC-2, and JSCE-2007. Nevertheless, ACI 318-19 prediction is conservative.

References

[1] "ACI 318-19 Building Code Requirements for Structural Concrete and Commentary," *Concrete*. 2019, doi: 10.14359/51716937.

[2] The European Union Per Regulation, "Eurocode 2: Design of concrete structures," 2004.

[3] C. STANDARDS and ASSOCIATION, *Design of concrete structures*. 2004.

[4] Ministry of Housing, *ECP 203-2017, Egyptian Building Code for Structural Concrete Design and Construction.* 2017.

[5] Japan Society of Civil Engineers., "JSCE., Standard specifications for concrete structure design.," 2007.

[6] J. L. Clarke and F. K. Birjandi, "Punching shear resistance of lightweight aggregate concrete slabs," *Mag. Concr. Res.*, vol. 42, no. 152, pp. 171–176, 1990.

[7] J.-J. Kim, J.-H. Moon, and K.-S. Youm, "Experimental Evaluation of the Punching Shear Strength with Lightweight Aggregate Concrete Slabs," *J. Korea Concr. Inst.*, vol. 26, no. 3, pp. 361–367, 2014.

[8] M. Osman, H. Marzouk, and S. Helmy, "Behavior of high-strength lightweight concrete slabs under punching loads," *Struct. J.*, vol. 97, no. 3, pp. 492–498, 2000.

[9] S. Sahoo and B. Singh, "Punching shear capacity of recycled-aggregate concrete slab-column connections," *J. Build. Eng.*, vol. 41, no. August 2020, p. 102430, 2021, doi: 10.1016/j.jobe.2021.102430.

[10] T. Urban, M. Gołdyn, Ł. Krawczyk, and Ł. Sowa, "Experimental investigations on punching shear of lightweight aggregate concrete flat slabs," *Eng. Struct.*, vol. 197, 2019, doi: 10.1016/j.engstruct.2019.109371.

[11] Q. Liu, B. Li, J. Xiao, and A. Singh, "Utilization potential of aerated concrete block powder and clay brick powder from C&D waste," *Constr. Build. Mater.*, vol. 238, p. 117721, 2020, doi: 10.1016/j.conbuildmat.2019.117721.

[12] K. Afshinnia and A. Poursaee, "The potential of ground clay brick to mitigate Alkali-Silica Reaction in mortar prepared with highly reactive aggregate," *Constr. Build. Mater.*, vol. 95, pp. 164–170, 2015, doi: 10.1016/j.conbuildmat.2015.07.155.

[13] C. L. Wong, K. H. Mo, S. P. Yap, U. J. Alengaram, and T. C. Ling, "Potential use of brick waste as alternate concrete-making materials: A review," *J. Clean. Prod.*, vol. 195, pp. 226–239, 2018, doi: 10.1016/j.jclepro.2018.05.193.

[14] H. Cheng, "Reuse Research Progress on Waste Clay Brick," *Procedia Environ. Sci.*, vol. 31, pp. 218–226, 2016, doi: 10.1016/j.proenv.2016.02.029.

[15] Ali A. Akhtaruzzaman and Abdul Hasnat, "Properties of Concrete Using Crushed Brick as Aggregate," *Concr. Int.*, vol. 5, no. 2, pp. 58–63, 1983.

[16] L. Zong, Z. Fei, and S. Zhang, "Permeability of recycled aggregate concrete containing fly ash and clay brick waste," *J. Clean. Prod.*, vol. 70, no. May 2014, pp. 175–182, 2014, doi: 10.1016/j.jclepro.2014.02.040.

[17] B. J. Odero, R. N. Mutuku, and C. K. Kabubo, "Engineering Mechanical Characteristics of Normal Concrete Partially Replaced With Crushed," *Int. J. Civ. Eng. Technol.*, vol. 6, no. 1, pp. 62–75, 2015.

[18] R. Kasi and P. Malasani, "Usage of Recycled Brick as Coarse Aggregate in Concrete," *Int. Adv. Res. J. Sci. Eng. Technol.*, vol. 3, no. 9, pp. 95–100, 2016, doi: 10.17148/IARJSET.2016.3918.

[19] A. A. Bashandy, F. M. Eid, and E. H. Abdou, "Lightweight Concrete Cast Using Recycled Aggregates," *Int. J. Constr. Eng. Manag.*, vol. 6, no. 2, pp. 35–45, 2017, doi: 10.5923/j.ijcem.20170602.01.

[20] A. Wongsa, V. Sata, P. Nuaklong, and P. Chindaprasirt, "Use of crushed clay brick and pumice aggregates in lightweight geopolymer concrete," *Constr. Build. Mater.*, vol. 188, pp. 1025–1034, 2018, doi: 10.1016/j.conbuildmat.2018.08.176.

[21] W. I. Khalil, Q. J. Frayyeh, and M. F. Ahmed, "Evaluation of sustainable metakaolin-geopolymer concrete with crushed waste clay brick," *IOP Conf. Ser. Mater. Sci. Eng.*, vol. 518, no. 2, 2019, doi: 10.1088/1757-899X/518/2/022053.

[22] H. Adem, E. Athab, S. Thamer, and A. T. Jasim, "The behavior of Lightweight Aggregate Concrete Made with Different Types of Crushed Bricks," *IOP Conf. Ser. Mater. Sci. Eng.*, vol. 584, no. 1, 2019, doi: 10.1088/1757-899X/584/1/012040.

[23] P. T. Bui, X. N. Nguyen, M. N. Tang, Y. Ogawa, and K. Kawai, *Effects of Amounts and Moisture States of Clay-Brick Waste as Coarse Aggregate on Slump and Compressive Strength of Concrete*, vol. 54. Springer Singapore, 2020.

[24] A. R. Khaloo, "Properties of concrete using crushed clinker brick as coarse aggregate," *ACI Mater. J.*, vol. 91, no. 4, pp. 401–407, 1994, doi: 10.14359/4058.

[25] C. S. Poon and D. Chan, "Feasible use of recycled concrete aggregates and crushed clay brick as unbound road sub-base," *Constr. Build. Mater.*, vol. 20, no. 8, pp. 578–585, 2006, doi: 10.1016/j.conbuildmat.2005.01.045.

[26] F. M. Khalaf, "Using crushed clay brick as coarse aggregate in concrete," *J. Mater. Civ. Eng.*, vol. 18, no. 4, pp. 518–526, 2006, doi: 10.1061/(ASCE)0899-1561(2006)18:4(518).

[27] F. S. Kallak, "Use Of Crushed Bricks As Coarse Aggregate In Concrete," *Tikrit J. Eng. Sci.*, vol. 16, no. 3, pp. 64–70, 2009.

[28] J. Yang, Q. Du, and Y. Bao, “Concrete with recycled concrete aggregate and crushed clay bricks,” *Constr. Build. Mater.*, vol. 25, no. 4, pp. 1935–1945, 2011, doi: 10.1016/j.conbuildmat.2010.11.063.

[29] S. Ishtiaq Ahmad and S. Roy, “Creep Behavior and Its Prediction for Normal Strength Concrete Made from Crushed Clay Bricks as Coarse Aggregate,” *J. Mater. Civ. Eng.*, vol. 24, no. 3, pp. 308–314, 2012, doi: 10.1061/(ASCE)MT.1943-5533.0000391.

[30] N. M. Ibrahim, S. Salehuddin, R. C. Amat, N. L. Rahim, and T. N. T. Izhar, “Performance of Lightweight Foamed Concrete with Waste Clay Brick as Coarse Aggregate,” *APCBEE Procedia*, vol. 5, pp. 497–501, 2013, doi: 10.1016/j.apcbee.2013.05.084.

[31] A. Mobili, C. Giosuè, V. Corinaldesi, and F. Tittarelli, “Bricks and concrete wastes as coarse and fine aggregates in sustainable mortars,” *Adv. Mater. Sci. Eng.*, vol. 2018, 2018, doi: 10.1155/2018/8676708.

[32] D. David, B. Sebastian, and M. A. Johny, “Partial Replacement of Fine Aggregate with Crushed Clay Brick in Cellular Concrete,” *Innov. Res. Sci. Eng. Technol.*, vol. 6, no. 5, pp. 8218–8226, 2017, doi: 10.15680/IJIRSET.2017.0605161.

[33] Z. Ge, Z. Gao, R. Sun, and L. Zheng, “Mix design of concrete with recycled clay-brick-powder using the orthogonal design method,” *Constr. Build. Mater.*, vol. 31, pp. 289–293, 2012, doi: 10.1016/j.conbuildmat.2012.01.002.

[34] A. Heidari and B. Hasanpour, “Effects of waste bricks powder of gachsaran company as a pozzolanic material in concrete,” *Asian J. Civ. Eng.*, vol. 14, no. 5, pp. 755–763, 2013.

[35] A. Schackow, D. Stringari, L. Senff, S. L. Correia, and A. M. Segadães, “Influence of fired clay brick waste additions on the durability of mortars,” *Cem. Concr. Compos.*, vol. 62, pp. 82–89, 2015, doi: 10.1016/j.cemconcomp.2015.04.019.

[36] D. L. Summerbell, C. Y. Barlow, and J. M. Cullen, “Potential reduction of carbon emissions by performance improvement: A cement industry case study,” *J. Clean. Prod.*, vol. 135, pp. 1327–1339, 2016, doi: 10.1016/j.jclepro.2016.06.155.

[37] M. F. Zawrah, R. A. Gado, N. Feltin, S. Ducourtieux, and L. Devoille, “Recycling and utilization assessment of waste fired clay bricks (Grog) with granulated blast-furnace slag for geopolymer production,” *Process Saf. Environ. Prot.*, vol. 103, no. July 2018, pp. 237–251, 2016, doi: 10.1016/j.psep.2016.08.001.

[38] P. Srinivas, A. S. S. V. Prasad, and S. A. Kumar, “Experimental Study on Strength of Concrete with Partial Replacement of Fine Aggregate with Waste,” *Int. J. Adv. Res. Ideas Innov. Technol.*, vol. 2, no. 8, pp. 2–5, 2016.

[39] J. M. Ortega, V. Letelier, C. Solas, G. Moriconi, M. Á. Climent, and I. Sánchez,

"Long-term effects of waste brick powder addition in the microstructure and service properties of mortars," *Constr. Build. Mater.*, vol. 182, pp. 691–702, 2018, doi: 10.1016/j.conbuildmat.2018.06.161.

[40] V. Letelier, J. M. Ortega, P. Muñoz, E. Tarela, and G. Moriconi, "Influence of Waste brick powder in the mechanical properties of recycled aggregate concrete," *Sustain.*, vol. 10, no. 4, pp. 1–16, 2018, doi: 10.3390/su10041037.

[41] C. Zheng, C. Lou, G. Du, X. Li, Z. Liu, and L. Li, "Mechanical properties of recycled concrete with demolished waste concrete aggregate and clay brick aggregate," *Results Phys.*, vol. 9, pp. 1317–1322, 2018, doi: 10.1016/j.rinp.2018.04.061.

[42] J. Shao, J. Gao, Y. Zhao, and X. Chen, "Study on the pozzolanic reaction of clay brick powder in blended cement pastes," *Constr. Build. Mater.*, vol. 213, pp. 209–215, 2019, doi: 10.1016/j.conbuildmat.2019.03.307.

[43] Z. Duan, S. Hou, J. Xiao, and B. Li, "Study on the essential properties of recycled powders from construction and demolition waste," *J. Clean. Prod.*, vol. 253, 2020, doi: 10.1016/j.jclepro.2019.119865.

[44] M. M. Atyia, M. G. Mahdy, and M. Abd Elrahman, "Production and properties of lightweight concrete incorporating recycled waste crushed clay bricks," *Constr. Build. Mater.*, vol. 304, p. 124655, 2021.

[45] F. Debieb and S. Kenai, "The use of coarse and fine crushed bricks as aggregate in concrete," *Constr. Build. Mater.*, vol. 22, no. 5, pp. 886–893, 2008, doi: 10.1016/j.conbuildmat.2006.12.013.

[46] M. Abdur, T. Hossain, and M. A. Islam, "Properties of higher strength concrete made with crushed brick as coarse aggregate," *J. Civ. Eng.*, vol. 37, no. 1, pp. 43–52, 2009.

[47] Y. Zhao, J. Gao, F. Chen, C. Liu, and X. Chen, "Utilization of waste clay bricks as coarse and fine aggregates for the preparation of lightweight aggregate concrete," *J. Clean. Prod.*, vol. 201, pp. 706–715, 2018, doi: 10.1016/j.jclepro.2018.08.103.

[48] ACI 213R-2014, *213R-14 Guide for Structural Lightweight-Aggregate Concrete*. 2014.